



## Electrodeposition of tungsten from $\text{ZnCl}_2\text{-NaCl-KCl-KF-WO}_3$ melt and investigation on tungsten species in the melt

Koji Nitta<sup>a,b,\*</sup>, Toshiyuki Nohira<sup>a,\*\*,1</sup>, Rika Hagiwara<sup>a</sup>, Masatoshi Majima<sup>b</sup>, Shinji Inazawa<sup>b</sup>

<sup>a</sup> Department of Fundamental Energy Science, Graduate School of Energy Science, Kyoto University, Sakyo-ku, Kyoto 606-8501, Japan

<sup>b</sup> Electronics & Materials R&D Labs, Sumitomo Electric Industries, Ltd., 1-1-3, Shimaya, Konohana-ku, Osaka 554-0024, Japan

### ARTICLE INFO

#### Article history:

Received 31 May 2009

Received in revised form 7 October 2009

Accepted 8 October 2009

Available online 10 November 2009

#### Keywords:

Molten salt

$\text{ZnCl}_2\text{-NaCl-KCl}$

Electrodeposition

Tungsten

Tungsten oxide

### ABSTRACT

The electrodeposition of tungsten in  $\text{ZnCl}_2\text{-NaCl-KCl-KF-WO}_3$  melt at 250 °C was further studied to obtain a thicker deposit. In the ordinary electrolysis at 0.08 V vs.  $\text{Zn(II)/Zn}$ , the current density decreased from 1.2  $\text{mA cm}^{-2}$  to 0.3  $\text{mA cm}^{-2}$  in 6 h. A thickness of the obtained tungsten layer was 2.1  $\mu\text{m}$  and the estimated current efficiency was 93%. A supernatant salt and a bottom salt were sampled after 6 h from the melting and were analyzed by ICP-AES and XRD. It was found that the soluble tungsten species slowly changes to insoluble ones in the melt. The soluble species was suggested to be  $\text{WO}_3\text{F}^-$  anion. One of the insoluble species was confirmed to be  $\text{ZnWO}_4$  and the other one was suggested to be  $\text{K}_2\text{WO}_2\text{F}_4$ . Electrodeposition was carried out under the same condition as above except for the intermittent addition of  $\text{WO}_3$  every 2 h. The current density was kept at the initial value and the thickness was 4.2  $\mu\text{m}$ . The intermittent addition of  $\text{WO}_3$  was confirmed to be effective to obtain a thicker tungsten film.

© 2009 Elsevier Ltd. All rights reserved.

### 1. Introduction

Micro-parts for micro-electro-mechanical systems (MEMS) are becoming increasingly important, and the lithographic galvanofarming abformung (LIGA) process for producing such parts is attracting attention [1]. The LIGA process is already used in practical applications [2,3], and holds great promise for the future. The current LIGA process, however, requires electroforming in an aqueous solution, and thus the applicable materials are restricted to copper, gold, nickel, Ni-Fe alloys and Ni-Co alloys [4–9]. Nevertheless, the strength and durability of the materials used in the micro-parts are expected to be improved, wherein refractory metals (especially tungsten) have the greatest potential.

Although the electrodeposition of tungsten from an aqueous solution is extremely difficult, Senderoff and Mellors obtained electrodeposits of refractory metals from alkali metal fluoride melts at 700–850 °C [10,11], and Katagiri et al. successfully electrodeposited metallic tungsten from  $\text{ZnBr}_2\text{-NaBr}$  [12] and  $\text{ZnCl}_2\text{-NaCl}$  [13] at 350–450 °C. However, the resist sheet for the LIGA process deteriorates at such high temperatures (350 °C or more). We have therefore been investigating tungsten electrodeposition in a

temperature range in which the resist is not deformed. We have already reported that electrodeposition of tungsten is possible in a  $\text{ZnCl}_2\text{-NaCl-KCl}$  melt (mp 203 °C) at 250 °C using  $\text{WCl}_4$  as the tungsten ion source, and that the addition of KF to the melt gives the smoother deposits probably owing to the change of ligand structure of the tungsten complex ions in the melt [14]. Furthermore, we reported that the usage of  $\text{WO}_3$  as a tungsten ion source gives smoother and denser deposits, and that it is possible to coat conventional LIGA parts with tungsten [15]. In addition to the higher quality of the deposit,  $\text{WO}_3$  has another advantage of non-volatility compared with  $\text{WCl}_4$  that is volatile at 250 °C. However, the decrease of current during a long-term electrodeposition was found for the  $\text{ZnCl}_2\text{-NaCl-KCl-KF-WO}_3$  melt, which was a major obstacle in obtaining thicker tungsten deposits. So, in this study, we further studied the electrodeposition of tungsten and especially focused on tungsten species in the melt. The mechanism of the change of ionic species is discussed and a method to maintain the electrodeposition longer time is proposed.

### 2. Experimental

#### 2.1. Materials and apparatus

All the chemicals were anhydrous reagent grade.  $\text{ZnCl}_2$  (99.9%, Wako Pure Chemical Industries, Ltd.) was dried in a furnace under vacuum at 130 °C for three days or more. NaCl, KCl, KF (99% each, Wako Pure Chemical Industries, Ltd.) and  $\text{WO}_3$  (99.5%, Wako Pure Chemical Industries, Ltd.) were dried in a furnace under vacuum

\* Corresponding author. Tel.: +81 6 6466 5637; fax: +81 6 6466 5683.

\*\* Corresponding author. Tel.: +81 75 753 4817; fax: +81 75 753 5906.

E-mail addresses: [nitta-koji@sei.co.jp](mailto:nitta-koji@sei.co.jp) (K. Nitta), [nohira@energy.kyoto-u.ac.jp](mailto:nohira@energy.kyoto-u.ac.jp) (T. Nohira).

<sup>1</sup> ISE member.

at 400 °C for three days or more. The chemicals were thoroughly mixed ( $\text{ZnCl}_2:\text{NaCl}:\text{KCl}:\text{KF}:\text{WO}_3 = 0.6:0.2:0.2:0.04:0.0054$ , in mole fraction) in an alumina crucible on a heating plate in a glove box filled with argon. The salts were melted at 250 °C. The working electrode was a nickel plate (99.9%,  $10 \times 10 \times 0.2$  mm, Nilaco Corp.). The nickel plate was electrochemically polished in sulfuric acid beforehand. The counter electrode was a glassy carbon rod (3 mm in diameter, GC-20, Tokai Carbon Co., Ltd.). A zinc wire (99.99%, 0.5 mm in diameter, Nilaco Corp.) immersed in the melt was used as the reference electrode. A chromel–alumel thermocouple was used for the temperature measurement.

## 2.2. Electrolysis and evaluation of electrodeposits

The cyclic voltammetry and potentiostatic electrolysis were carried out using an electrochemical measurement system (Hokuto Denko Co., Ltd., HSV-100) in a glove box filled with argon. A schematic drawing of experimental apparatus has been shown elsewhere [14]. After the electrolysis, electrodes were immersed in distilled water to remove adherent salts. In order to evaluate the thickness of the film obtained, the cross-sectional view of deposits was observed by field emission scanning electron microscopy (FE-SEM, Hitachi S-800).

## 2.3. Analysis of the salts

The supernatant salt and the bottom salt containing precipitate were sampled after 6 h had passed from the melting. These samples were scraped from the cooled and solidified melt. The bottom salt was a mixture of the precipitate and the solidified melt. The compositions of Zn, K, Na and W in these samples were measured by inductively coupled plasma atomic emission spectrometry (ICP-AES, Thermo Fisher Scientific Inc., iCAP6500 DUO). The composition of F was measured by ion chromatography (IC, Dionex Corp., ICS-3000). In order to identify the bottom salt, it was sealed into a polyethylene bag under argon and analyzed by X-ray diffractometry (XRD, Rigaku Industrial Co., Ltd., RINT1500).

## 3. Results and discussion

### 3.1. Cyclic voltammetry, potentiostatic electrolysis and analysis of electrodeposited tungsten

A cyclic voltammogram (CV) was measured immediately after the salts ( $\text{ZnCl}_2\text{--NaCl--KCl--KF--WO}_3$ ) were melted at 250 °C, which is shown as a solid curve in Fig. 1. Cathodic currents were observed at more negative than 0.45 V vs. Zn (II)/Zn. According to our previous study [15], these cathodic currents correspond to the electrodeposition of tungsten. In the same melt, potentiostatic electrolysis was conducted for a nickel electrode at 0.08 V for 6 h. It has been clarified that electrodeposition of tungsten occurs without the codeposition of zinc at this potential [15]. Fig. 2 shows a change of current density during the electrolysis. In the first five minutes, current density decreased rapidly to  $1.0 \text{ mA cm}^{-2}$ . Then, it increased slightly from  $1.0 \text{ mA cm}^{-2}$  to  $1.2 \text{ mA cm}^{-2}$  in 30 min. After that, it decreased gradually to  $0.3 \text{ mA cm}^{-2}$  in 6 h. Since the decrease of current was observed, a CV was measured again after the potentiostatic electrolysis, which is shown as a dashed curve in Fig. 1. The current attributed to electrodeposition of tungsten decreased and the current assigned to the nickel–zinc alloy formation was observed at more negative than 0.05 V [14]. This cathodic current of nickel–zinc alloy formation was observed in the melt without  $\text{WO}_3$  [15]. Therefore, it is considered that the rate of tungsten electrodeposition became slow, and that the nickel–zinc alloy formation proceeded before the surface of electrode was covered with tungsten. Fig. 3

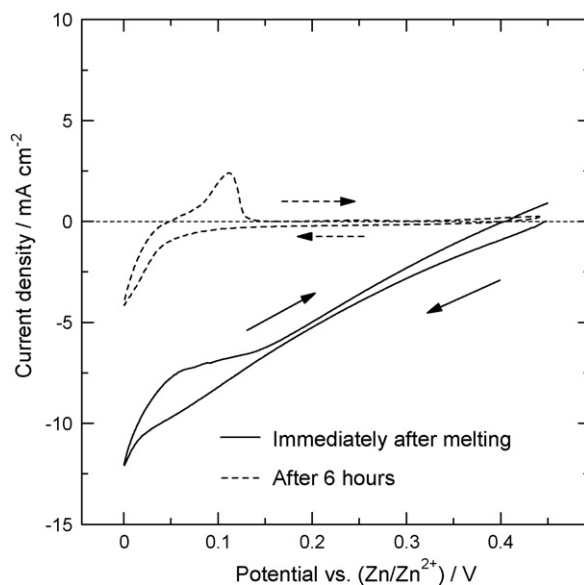


Fig. 1. Cyclic voltammograms for nickel electrodes in the  $\text{ZnCl}_2\text{--NaCl--KCl--KF--WO}_3$  melt at 250 °C. Solid curve: immediately after melting. Dashed curve: after potentiostatic electrolysis at 0.08 V vs. Zn (II)/Zn for 6 h. Scan rate:  $0.05 \text{ V s}^{-1}$ .

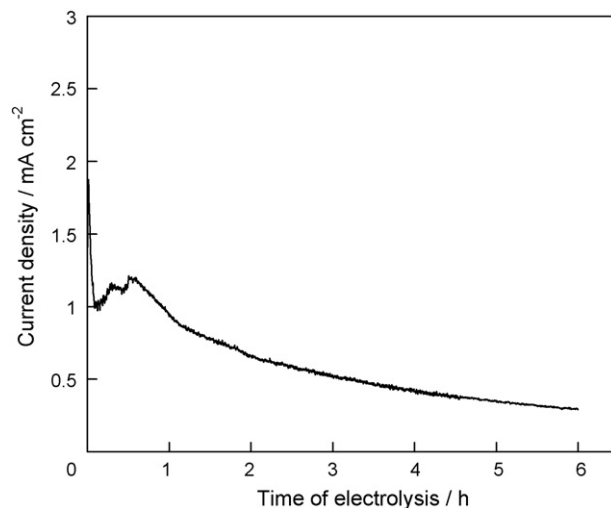


Fig. 2. A change of current density during the potentiostatic electrolysis at 0.08 V vs. Zn(II)/Zn for 6 h in the  $\text{ZnCl}_2\text{--NaCl--KCl--KF--WO}_3$  melt at 250 °C.

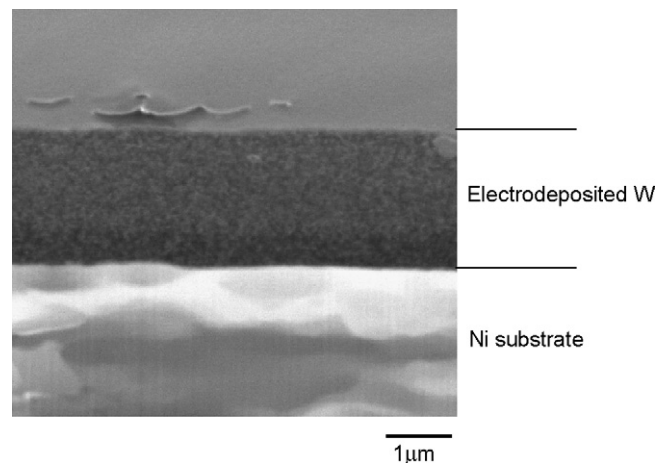
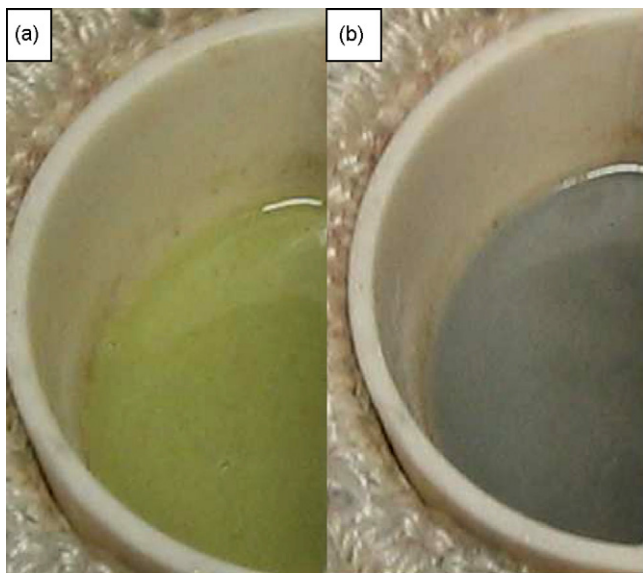


Fig. 3. A cross-sectional SEM image of electrodeposited tungsten by the potentiostatic electrolysis in the  $\text{ZnCl}_2\text{--NaCl--KCl--KF--WO}_3$  melt at 0.08 V vs. Zn(II)/Zn for 6 h at 250 °C.



**Fig. 4.** (a.) The appearance of the  $\text{ZnCl}_2\text{-NaCl-KCl-KF-WO}_3$  melt immediately after melted at  $250^\circ\text{C}$ . (b.) The appearance of the  $\text{ZnCl}_2\text{-NaCl-KCl-KF-WO}_3$  melt after 6 h from melting at  $250^\circ\text{C}$  (without electrolysis).

shows a cross-sectional SEM image of the electrodeposited tungsten. The thickness is approximately  $2.1\ \mu\text{m}$ . The current efficiency is calculated to be 93% from the thickness of the deposit, assuming that the electrodeposition proceeds via a six-electron reduction as follows.



Although the accuracy of this value is not very high due to the error in estimating the thickness, it is reasonable to consider that the electrodeposition proceeds by a six-electron reduction.

The reasons for the decrease and the increase of current are discussed. Firstly, it is considered that the rapid decrease in the first five minutes is mainly due to the decrease of tungsten species or the increase of oxide ions in the vicinity of working electrode. The slight current increase in the next half an hour indicates the increase of bulk concentration of W(VI) ion. It is assumed that the bulk concentration of W(VI) ion reached the highest value after about 0.5 h from the melting due to a time lag of  $\text{WO}_3$  dissolution. On the other hand, the moderate current decrease in 6 h is presumed to be caused by the decrease of bulk concentration of W(VI) ion. Since the amount of W(VI) ion consumed by the electrodeposition is calculated to be only 0.36% of the total amount of  $\text{WO}_3$  in the melt, the decrease of bulk concentration of W(VI) ion was not caused by the electrodeposition. Furthermore, the decrease of W(VI) ions was not caused by volatilization of tungsten compounds because very little sublimate was observed on the top of the vessel and tungsten was not detected from the sublimate by XPS analysis. Thus, it is considered that the decrease of W(VI) ions is caused by the transformation of the electrochemically active tungsten species to inactive ones.

### 3.2. The analysis of the melts by ICP-AES, IC and XRD

The appearance of the melt immediately after melted at  $250^\circ\text{C}$  is shown in Fig. 4-a. The melt was yellow and not transparent. After 6 h without electrolysis, the melt became transparent, as shown in Fig. 4-b, and a gray precipitate was observed in the bottom of the crucible. Then, the compositions of Zn, K, Na and W in the bottom salt and the supernatant salt were analyzed by ICP-AES, and those of F were analyzed by IC. These results are listed in Table 1. The data has been standardized so that the composition of Zn becomes 60.0 for all cases. The composition of tungsten in the supernatant

**Table 1**

Compositions for the designed salt, the supernatant salt and the bottom salt including a precipitate. The salt was sampled after 6 h from the melting.

	Na	K	Zn	W	F
Designed salt/mol ratio	20.0	24.0	60.0	0.54	4.0
Supernatant salt/mol ratio	19.7	23.9	60.0	0.06	3.9
Bottom salt/mol ratio	18.5	22.2	60.0	7.2	5.2

salt is lower compared with the designed value. On the other hand, the tungsten content in the bottom salt is higher than the designed one. It is also seen that the composition of F in the bottom salt is high. From these results, the following three facts were found: (i) A soluble tungsten species is generated upon melting. (ii) The soluble species slowly changes to insoluble tungsten species. (iii) The insoluble species contains fluorine. It is also confirmed that the decrease of current during the electrodeposition was caused by the decrease of soluble tungsten species in the melt.

To investigate the tungsten species in the bottom salt, the sampled salt was analyzed by XRD. The obtained spectrum is shown in Fig. 5. Peaks at  $22.7^\circ$ ,  $23.9^\circ$  and  $36.1^\circ$  are assigned to a polyethylene bag that was used to seal the hygroscopic salt. Other peaks are mostly assigned to  $\text{ZnWO}_4$ , but several peaks remain unidentified. These unidentified peaks may be due to a tungsten compound of which crystal structure has not been reported yet. Moreover, no peaks of  $\text{ZnCl}_2$ , NaCl and KCl are observed, although they are the main components of the melt. It is likely that the solidified salt exists in an amorphous phase. In our previous study [16], the ideal glass transition temperature of the  $\text{ZnCl}_2\text{-NaCl-KCl}$  eutectic melt was determined to be  $10^\circ\text{C}$  from VTF plots of viscosity and ionic conductivity, which is consistent with the result of XRD. Such glass forming behavior of the melt should be related with the formation of chlorozincate anions like  $\text{Zn}_2\text{Cl}_5^-$  and  $\text{ZnCl}_3^-$  [17].

### 3.3. Discussion on the change of the tungsten species

In our previous study [15], it has been found that  $\text{F}^-$  ions are necessary to dissolve  $\text{WO}_3$  in the melt. Thus, the soluble tungsten species, which is generated immediately after melting, should contain  $\text{F}^-$  ions. According to the literature [18], many tungsten compounds containing chlorine or fluorine are volatile at  $250^\circ\text{C}$ . On the other hand, the tungsten species in this system is not volatile as described in section 3.1. Thus, it is considered that the soluble tungsten species is  $\text{WO}_3\text{F}^-$  anion.

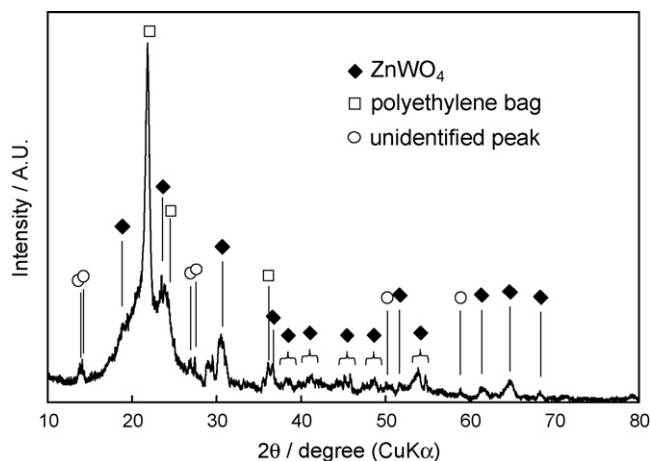


**Fig. 5.** An XRD spectrum of the bottom salt of the  $\text{ZnCl}_2\text{-NaCl-KCl-KF-WO}_3$  melt after 6 h from melting at  $250^\circ\text{C}$ .

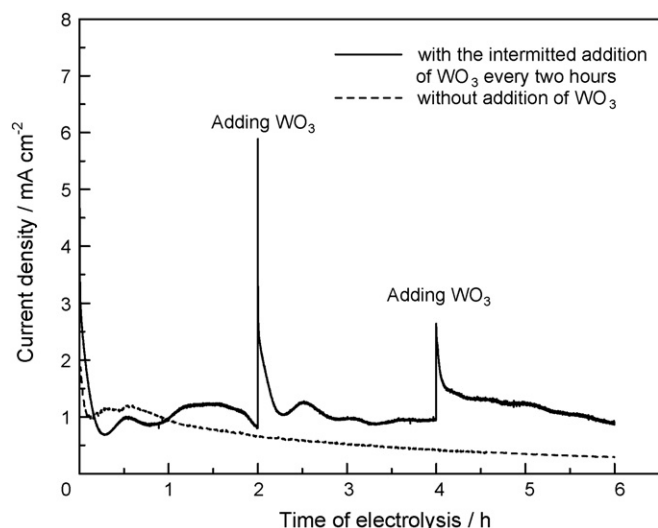
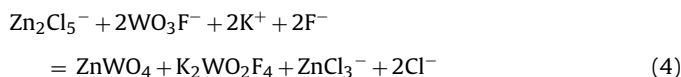


**Fig. 6.** A change of current density during the potentiostatic electrolysis in the  $\text{ZnCl}_2\text{-NaCl-KCl-KF-WO}_3$  melt at 0.08 V vs.  $\text{Zn(II)/Zn}$  for 6 h with the intermitted addition of  $\text{WO}_3$  every 2 h at 250 °C.

Then, a reaction of tungsten electrodeposition is written as



On the other hand, it is predicted that  $\text{WO}_3\text{F}^-$  anions slowly change into insoluble  $\text{ZnWO}_4$ . Considering that both zinc and oxygen are necessary to transform  $\text{WO}_3\text{F}^-$  to  $\text{ZnWO}_4$ , and that the precipitate should also contain fluorine, the following reaction is suggested.



Here, the unidentified peaks in Fig. 5 are considered to correspond to  $\text{K}_2\text{WO}_2\text{F}_4$ . The moderate decrease of current during the potentiostatic electrolysis can be explained by the decrease of  $\text{WO}_3\text{F}^-$  anion according to reaction (4).

### 3.4. A method to maintain the electrodeposition for a longer period

From the above discussion, the slow transformation of soluble tungsten species to insoluble ones was suggested to be the main reason for the current decrease. However, according to the current decay curve in Fig. 2, the current density is relatively high in the initial 2 h. So, it is expected that the electrodeposition proceeds for a longer period by adding  $\text{WO}_3$  every 2 h. To confirm this, electrodeposition was conducted under the same condition as Fig. 2 except for the addition of  $\text{WO}_3$  every 2 h. The amount of  $\text{WO}_3$  in every addition was the same as the initial amount. The current response is shown in Fig. 6 together with the case of no intermittent addition. A sharp increase of the current is observed at every addition and the average current is maintained at the same level as the initial 2 h. Fig. 7 shows a cross-sectional view of the electrodeposited tungsten. The thickness of tungsten layer was approximately 4.2  $\mu\text{m}$  and the current efficiency was calculated to be 90%. So, it is confirmed that the intermittent addition of  $\text{WO}_3$  is effective to maintain the current density at a high level for a long period, which enables us to obtain a thicker tungsten film.

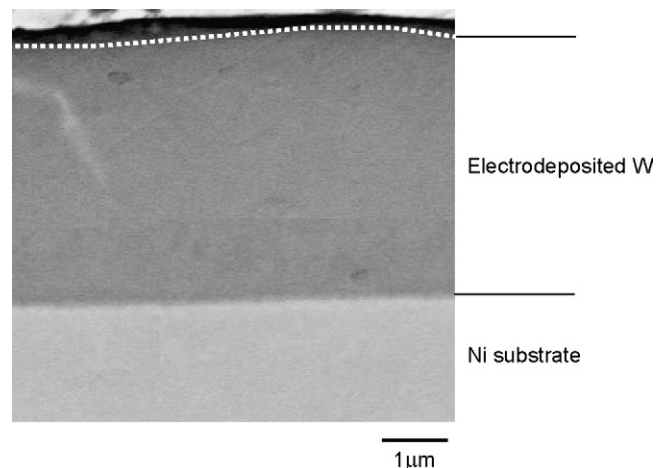


**Fig. 7.** A cross-sectional SEM image of the electrodeposited tungsten by the potentiostatic electrolysis in the  $\text{ZnCl}_2\text{-NaCl-KCl-KF-WO}_3$  melt at 0.08 V vs.  $\text{Zn(II)/Zn}$  for 6 h with the intermitted addition of  $\text{WO}_3$  every 2 h at 250 °C.

## 4. Conclusions

A cause of the current decay was revealed for the electrodeposition of tungsten in the  $\text{ZnCl}_2\text{-NaCl-KCl-KF-WO}_3$  melt at 250 °C. It was found that the soluble tungsten species slowly changes to insoluble ones. The soluble species was suggested to be  $\text{WO}_3\text{F}^-$  anion. One of the insoluble species was confirmed to be  $\text{ZnWO}_4$  and the other one was suggested to be  $\text{K}_2\text{WO}_2\text{F}_4$ . The intermittent addition of  $\text{WO}_3$  every 2 h was confirmed to be effective to maintain the current density at a high level, which enables to obtain a thicker tungsten film.

## Acknowledgments

This study was partly supported by Industrial Technology Research Grant Program in 2003 from the New Energy and Industrial Technology Development Organization (NEDO) of Japan.

## References

- [1] Y. Hirata, Nucl. Instrum. Methods B 208 (2003) 21.
- [2] T. Haga, K. Okada, J. Yorita, Y. Hirata, S. Shimada, ICEP Proceedings, 2002, p. 421.
- [3] Y. Hirata, H. Nakaishi, T. Numazawa, H. Takada, IEEE Ultrasonics Symposium Proceedings 2, 1997, p. 877.
- [4] E.W. Becker, W. Ehrfeld, P. Haggmann, A. Maner, D. Münchmeyer, Microelectron. Eng. 4 (1986) 35.
- [5] A. Rogner, J. Eicher, D. Münchmeyer, R.-P. Peters, J. Mohr, J. Micromech. Microeng. 2 (1992) 133.
- [6] J. Hormes, J. Göttert, K. Lian, Y. Desta, L. Jian, Nucl. Instrum. Methods Phys. Res. B 199 (2003) 332.
- [7] L. Singleton, J. Photopolym. Sci. Technol. 16 (2003) 413.
- [8] S. Sugiyama, Proc. SPIE 5062 (2003) 821.
- [9] D. Golodnitsky, N. Gudim, G. Volyanyuk, Plat. Surf. Finish. 2 (1998) 65.
- [10] S. Senderoff, G.W. Mellors, Science 153 (1966) 1475.
- [11] S. Senderoff, G.W. Mellors, J. Electrochem. Soc. 114 (1967) 586.
- [12] A. Katagiri, M. Suzuki, Z. Takehara, J. Electrochem. Soc. 138 (1991) 767.
- [13] M. Masuda, H. Takenishi, A. Katagiri, J. Electrochem. Soc. 148 (2001) C59.
- [14] H. Nakajima, T. Nohira, R. Hagiwara, Electrochem. Solid-State Lett. 8 (7) (2005) C91.
- [15] H. Nakajima, T. Nohira, R. Hagiwara, K. Nitta, S. Inazawa, K. Okada, Electrochim. Acta 53 (2007) 24.
- [16] K. Nitta, T. Nohira, R. Hagiwara, M. Majima, S. Inazawa, Electrochim. Acta 54 (2009) 4898.
- [17] J.J. Watkins, E.C. Ashby, Inorg. Chem. 13 (1974) 2350.
- [18] J. Canterford, R. Colton, Halides of the Transition Elements: Halides of the second and third Row Transition Metals, vol. 208, Wiley, New York, 1968.